Photoelectron Imaging and Theoretical Calculations of Bimetallic Clusters: AgCu−, AgCu2−, and Ag2Cu−

ARTICLE *in* THE JOURNAL OF PHYSICAL CHEMISTRY A · OCTOBER 2012

Impact Factor: 2.69 · DOI: 10.1021/jp307478x · Source: PubMed

THE JOURNAL OF PHYSICAL CHEMISTRY A

Article

pubs.acs.org/JPCA

Photoelectron Imaging and Theoretical Calculations of Bimetallic Clusters: $AgCu^-$, $AgCu_2^-$, and Ag_2Cu^-

Hua Xie,[†] Xiaoyi Li,[‡] Lijuan Zhao,[‡] Zhengbo Qin,[†] Xia Wu,[†] Zichao Tang,*[,†] and Xiaopeng Xing*[,‡]

[†]State Key Laboratory of Molecular Reaction Dynamics, Dalian Institute of Chemical Physics, Chinese Academy of Sciences, Dalian 116023, China

[‡]Graduate University of Chinese Academy of Sciences, College of Materials Sciences and Opto-Electronic Technology, Beijing 100049, China

Supporting Information

ABSTRACT: Bimetallic clusters of $AgCu^-$, $AgCu_2^-$, and Ag_2Cu^- are investigated by using photoelectron imaging and theoretical calculations. Their photoelectron spectra have been obtained at the wavelength of 355 nm and that of $AgCu^-$ is also acquired at 1064 nm. The ground state vertical detachment energies of these three clusters are measured to be 0.96 (1), 2.39 (5), and 2.41 (5) eV. The ground state adiabatic detachment energy of $AgCu^-$ is measured to be 0.93 (1) eV. Other spectroscopic constants of $AgCu^-$ including its frequency, bond length, and dissociation energy (relative to the products Ag^- and Cu) are determined to be 191(15) cm^{-1}, 2.487(10) Å, and 1.39 eV according to its spectrum at 1064 nm. Only upper limits of the ground state adiabatic detachment energies of $AgCu_2^-$ and Ag_2Cu^- are estimated by using their spectra at 355 nm. The structures and properties of $AgCu^-$, $AgCu_2^-$, Ag_2Cu^-, and their neutral counterparts are also computed by using a strategy where the structural optimizations are performed with the PW91PW91 method and the energy calculations are performed with the CCSD (T) method. The calculations are in better agreement with the experiments than most of the previous theoretical work.

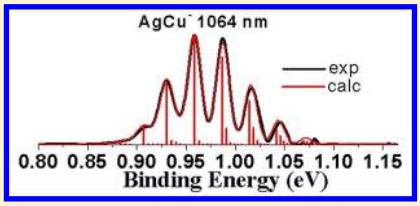

1. INTRODUCTION

There is a growing interest in bimetallic clusters[1−9] since mixing of different elements provides an important approach to manipulate their structures and properties. Coinage metal clusters have potential applications ranging from catalysis to optics and those containing more than one kind of coinage metal elements have attracted attention for a long time.[10−15] Studies on their dimers or trimers in the gas phase can reveal important characteristics which could also exist on the large sizes.

The dissociation energy and vibrational frequency of AgCu were first studied by using mass spectroscopy and thermo emission spectroscopy in the 1960s.[16,17] With the appearance of laser technique, more molecular constants were measured precisely by using resonant two-photon ionization spectroscopy.[13] The experiments with this laser spectroscopy also predicted the bond length of AgCu and the excitation energy of a high singlet state. In the subsequent works, the ionization potential of AgCu was measured by using threshold photoionization spectroscopy[18] and the charge-transfer bracketing method.[19] Additionally, the lumenscence spectroscopy has been used to study mass-selected AgCu in argon matrices,[20] in which the value of frequency was found to be consistent with the gas-phase observations. The resonant two-photon ionization spectroscopy and the charge-transfer bracketing method were also used to study the neutral trimers in the gas phase,[14] where the structures of their ground states, their ionization potential, and the properties of several excited states were reported. In contrast to the extensive experiments focusing on these neutral or cationic clusters containing silver and copper, important properties of their anions such as vertical detachment energy (VDE) and adiabatic detachment energy (ADE) have never been measured with experiments. At the same time, the bimetallic clusters of silver and copper were extensively studied by using different theoretical methods.[12,15,21−24] Many parameters of their anions were predicted even when there were no values from experiments to be compared with.

In this work, we report studies of $AgCu^-$, $AgCu_2^-$, and Ag_2Cu^- using photoelectron imaging technique. Their VDEs and ADEs are estimated. The vibrational frequency, bond length, and dissociation energy of $AgCu^-$ are also reported. The structures of these bimetallic cluster anions and their neutral counterparts are studied by using a combination of two theoretical methods. The calculated results are in good agreement with the experimental ones. We find that many parameters of the bimetallic clusters such as VDEs, ADEs, and bond lengths lie between the corresponding values of homoatomic clusters of silver and copper.

2. EXPERIMENTAL AND COMPUTATIONAL METHODS

The experiment is performed by using an instrument with a laser ablation source, a time-of-flight (TOF) mass spectrometer, and a collinear velocity-map photoelectron imaging analyzer. The whole apparatus has been described elsewhere[25] and only a

Received: July 28, 2012
Revised: September 28, 2012
Published: October 1, 2012

brief outline is given below. The small bimetallic cluster anions are generated by laser vaporization of a target compressed from mixed powders of silver and copper. The nascent clusters are cooled and expanded into the source chamber with helium carrier gas. The typical stagnation pressure of the carrier gas is about 1−3 atm. These anionic clusters are then extracted perpendicularly by a −1.2 kV high-pulse voltage and analyzed by the TOF mass spectrometer. After separation in space, the anion clusters of interest are introduced into the photodetachment region and crossed with a laser beam. Two photon energies, 355 (3.496 eV) and 1064 nm (1.165 eV), are used for $AgCu^-$ and only that of 355 nm is used for the two trimers. Photoelectrons are analyzed by the collinear velocity-map photoelectron imaging analyzer, which is built according to a modified design of Eppink and Parker.[26] Finally, the electrons are mapped onto an image detector consisting of a microchannel plate (MCP) assembly and a phosphor screen. The positions of photoelectrons are recorded by a charge-coupled device (CCD) camera and one typical image is obtained by accumulating 50000−100000 laser shots at 10 Hz repetition rate.

The obtained raw image reveals the projection of the photoelectron density in the 3D laboratory frame onto the 2D imaging detector. The original 3D distribution is reconstructed by using the Basis Set Expansion (BASEX) inverse Abel transform method, and the photoelectron spectrum is acquired by integrating one central slice of the 3D distribution.[27] The spectrometer is calibrated by using the spectra of Ag^- and Au^- at 355 nm. Its velocity resolution ($\Delta v/v$) is less than 2.5%, corresponding to 50 meV at an electron kinetic energy (eKE) of 1 eV. The uncertainties of the experimental detachment energies are mainly caused by the restriction of this resolution. They are estimated by the product of the energy resolution and the kinetic energy of corresponding photoelectrons. According to the reconstructed photoelectron distribution, the anisotropy parameter β can be obtained. Its value ranges from −1 to +2, corresponding to perfectly perpendicular and parallel transitions, respectively.

The structures of $AgCu^-$, Ag_2Cu^-, $AgCu_2^-$, and their neutral counterparts are optimized by using the PW91PW91 method[28] with the generalized gradient approximation (GGA). The aug-cc-PVTZ-pp basis sets[29,30] are used for both Ag and Cu. This theoretical method has been shown to be suitable for clusters containing coinage metals in our recent work.[31,32] Optimizations of each cluster start from all possible structural candidates with full relaxation of all atoms' positions. Vibration analysis is implemented to make sure that the obtained ones are true minimum points. The properties of optimized structures including VDEs and ADEs are computed by using the CCSD (T) method[33] with the same basis sets. All theoretical works are performed with the Gaussian 09 program.[34]

3. EXPERIMENTAL RESULTS

Panels a and b of Figure 1 show the photoelectron imaging results of $AgCu^-$ at 355 and 1064 nm, respectively. The left column of each panel indicates the raw and reconstructed images and the photoelectron energy spectrum is on the right. The direction of laser polarization is indicated by a double arrow on each raw image. Two peaks labeled as X and A in Figure 1a are near 0.96 and 2.80 eV. The vibrational progression of the X band is clearly resolved in Figure 1b. The Franck−Condon simulation of this progression is performed on the original velocity-frame spectrum, using the

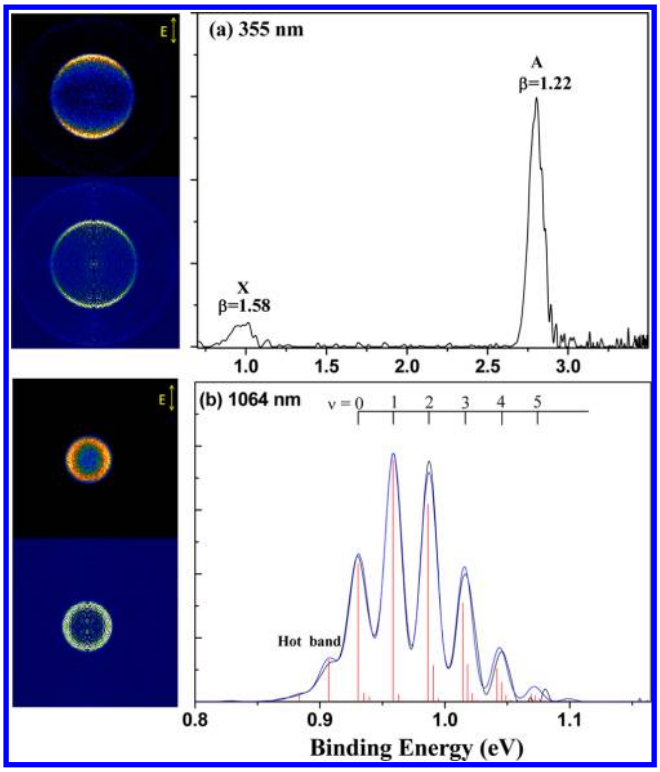

Figure 1. Photoelectron imaging results of $AgCu^-$ at (a) 355 nm (3.496 eV) and (b) 1064 nm (1.165 eV). The symmetric raw image (upper) and the reconstructed image (bottom) after inverse Abel transformations are shown on the left side of each panel. The double arrow on each raw image indicates the direction of the laser polarization. Photoelectron spectra are shown on the right side. The solid lines in both spectra stand for the experimental data. The anisotropy parameter β for each transition band is indicated in panel a and the vibrational progression and hot band of the first band are indicated in panel b. The blue line and red sticks in panel b come from Franck−Condon simulations.

PESCAL program[35] before transformation to electron binding energies, and the Morse Oscillator approximation is used for both AgCu and $AgCu^-$. The harmonic frequency and anharmonicity constant of AgCu were determined to be 231.8 cm^{-1} and 0.80 cm^{-1}, respectively.[17] Resonant two-photon ionization spectroscopy predicted the bond length of AgCu to be 2.373 Å.[13] With these three values fixed, the simulation obtains the result shown by the red sticks and blue curve in Figure 1b. The intensity of the experimental spectrum near 1.07−1.08 eV is very weak and the peak shape is abnormal. This could be caused by some limitations of our apparatus and data, which makes the weak signal in this range not be recorded and transformed precisely. Since the intensity of the theoretical curve near 1.07−1.08 eV is also very weak, the discrepancies in this range do not seriously affect the fitting results. The position of 0←0 transition, which stands for the adiabatic detachment energy of $AgCu^-$ or the electron affinity of AgCu, is determined to be 0.93(1) eV. The position of 1←0 transition, which stands for the vertical detachment energy of $AgCu^-$, is determined to be 0.96 (1) eV. The hot bands in the spectrum lead to determination of the frequency of $AgCu^-$, which is 191(15) cm^{-1}. According to the molecular orbital analysis, the extra electron of $AgCu^-$ tends to occupy an antibond σ orbital, which makes the bond of $AgCu^-$ longer than that of AgCu. The bond length of $AgCu^-$ is predicted to be 2.487(10) Å by simulation.

dx.doi.org/10.1021/jp307478x | J. Phys. Chem. A 2012, 116, 10365−10370

The spectra of $AgCu_2^-$ and Ag_2Cu^- at 355 nm are shown in panels a and b of Figure 2, respectively. Only one peak is

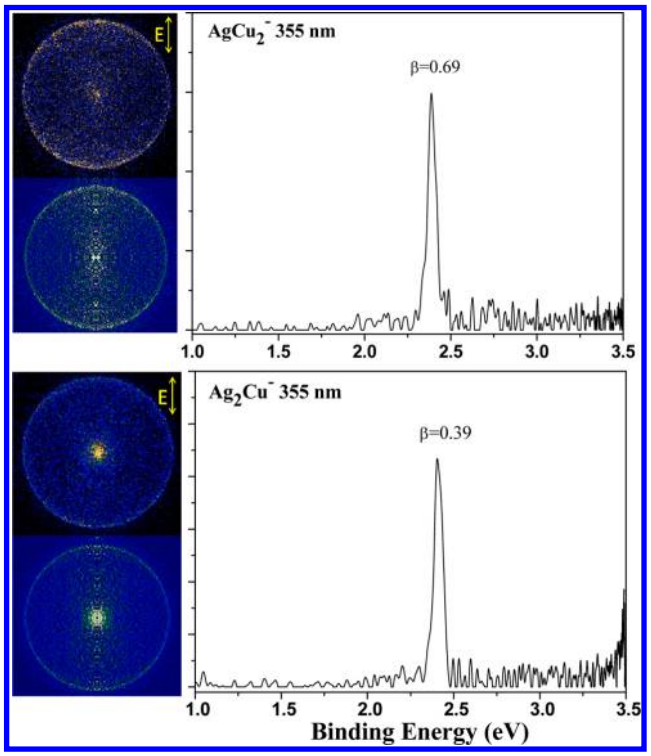

Figure 2. Photoelectron imaging results of (a) $AgCu_2^-$ and (b) Ag_2Cu^- at 355 nm (3.496 eV). The anisotropy parameter β for each transition band is indicated.

observed in each spectrum. The maximum of the peak (VDE) for $AgCu_2^-$ is 2.39(5) eV and that for Ag_2Cu^- is measured to be 2.41(5) eV. Both peaks seem asymmetric and have a slightly low-energy tail. This indicates that there could be geometry change between the ground state anion and that of the neutral. For both cases, the threshold of the main peak is taken as an upper limit for their ADE, which is 2.34 eV for $AgCu_2^-$ and 2.32 eV for Ag_2Cu^-.

The anisotropy parameters for the photoelectron bands of $AgCu^-$, $AgCu_2^-$, and Ag_2Cu^- at 355 nm are indicated in Figures 1 and 2. The relations between the detachment processes and the resulting PADs of anions are complicated and many theoretical efforts have been made to understand them. The qualitative s&p model developed by Sanov and co-workers can reasonably interpret the PADs of these small cluster anions.[36,37]

4. THEORETICAL RESULTS

Figure 3 displays calculated results of $AgCu^-$, $AgCu_2^-$, and Ag_2Cu^-. The structural parameters (bond length in Å and bond angle in deg) at the PW91PW91/aug-cc-PVTZ-pp level, the symmetries, the electronic states, and the relative energies (given in eV) at the CCSD (T)/aug-cc-PVTZ-pp level are shown for each structure. According the listed results, the ground states for $AgCu^-$ and AgCu are $^2\Sigma^+$ and $^1\Sigma^+$, respectively, and the first exited state of AgCu is $^3\Sigma^+$. The lowest-lying structure of $AgCu_2^-$ is $C_{\infty v}$ geometry ($^1\Sigma^+$) and the closest-lying isomer is $D_{\infty h}$ geometry ($^1\Sigma_g^+$). For the neutral $AgCu_2$, an acute triangle having C_s geometry ($^2A'$) is the lowest lying one. Similarly, anionic Ag_2Cu^- has two low-lying

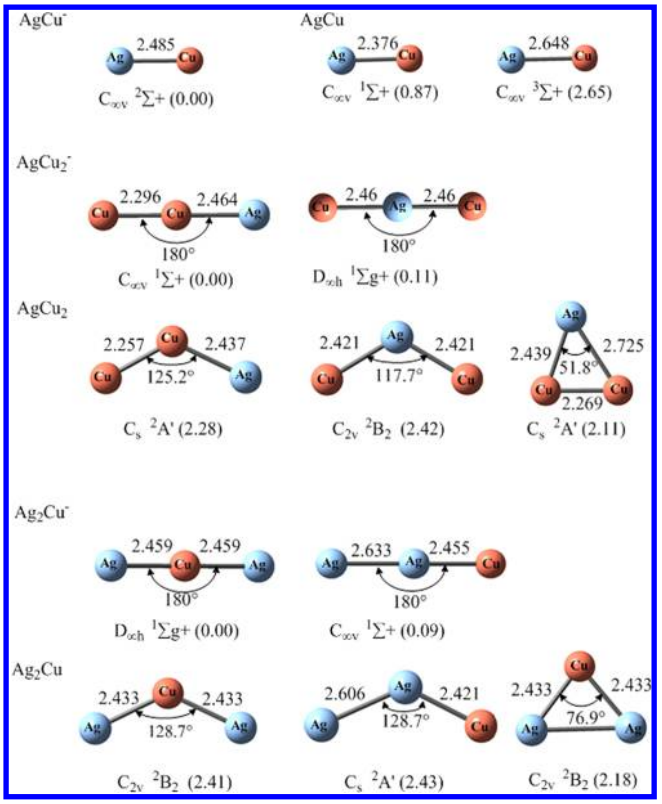

Figure 3. The theoretical results of $AgCu^-$, $AgCu_2^-$, Ag_2Cu^-, and their neutrals. The structural parameters (bond lengths in Å and bond angles in deg), the symmetries, the electronic states, and the energies relative to the anionic ground state (given in eV) are shown for each structure. The structural parameters are optimized by using PW91PW91 and the relative energies in parentheses are calculated by using CCSD (T) for structures optimized by PW91PW91.

structures of $D_{\infty h}$ ($^1\Sigma_g^+$) and $C_{\infty v}$ ($^1\Sigma^+$) and an acute triangle having C_{2v} geometry ($^2B_2$) is the lowest-lying one for Ag_2Cu.

According to the definitions, VDE is the energy difference between the anion and the neutral calculated at the equilibrium geometry of the anion, while ADE means the energy difference between the anion and its corresponding neutral at their respective equilibrium geometries. Theoretical VDEs and ADEs for these three clusters, those from previous theoretical studies,[12,15,38] and the above experimental ones are summarized in Table 1. Similarly, the theoretical bond lengths and the unscaled frequency values from vibration analysis of $AgCu^-$ $^2\Sigma^+$ and AgCu $^1\Sigma^+$ together with those of experimental values and previous researches[12,13,15,17,22−24,38,39] are summarized in Table 2.

5. DISCUSSION

5.1. $AgCu^-$. The frontier molecular orbitals in $AgCu^-$ originate from the interaction between atomic orbitals of Ag 5s and Cu 4s leading to the configuration of $AgCu^-$ $\sigma^2\sigma^{*1}$. The ground state of AgCu $^1\Sigma^+$ should be from $\sigma^2\sigma^{*0}$ and its first excited state $^3\Sigma^+$ should originate from $\sigma^1\sigma^{*1}$. Calculated results in Figure 3 indicate that the energies of AgCu $^1\Sigma^+$ and AgCu $^3\Sigma^+$ relative to the ground state of $AgCu^-$ $^2\Sigma^+$ are 0.87 and 2.65 eV. They are reasonably consistent with the threshold positions of X and A bands in Figure 1a.

The previous study with emission spectroscopy[13] revealed an excited state AgCu $^1\Sigma^+$ originating from excitation of the electron on the inner d subshells. This state is about 20800

dx.doi.org/10.1021/jp307478x | J. Phys. Chem. A 2012, 116, 10365−10370

Table 1. The Symmetries, Electronic States, Relative Energies, Adiabatic Detachment Energies (ADEs), and Vertical Detachment Energies (VDEs) of $AgCu^-$, $AgCu_2^-$, and Ag_2Cu^-[a]

cluster anion	ΔE (eV)	corresponding neutral	ADE (eV) calcd	ADE (eV) exptl	VDE (eV) calcd	VDE (eV) exptl
$AgCu^-$ $C_{\infty v}$ $^2\Sigma^+$	0	$C_{\infty v}$ $^1\Sigma^+$	0.87	0.93(1)	0.91	0.96(1)
			0.88[b]			
			0.81/0.72[c]			
Ag_2^- $D_{\infty h}$ $^2\Sigma_u^+$	0	$D_{\infty h}$ $^1\Sigma_g^+$		1.023(7)[d]		1.06(2)[d]
Cu_2^- $D_{\infty h}$ $^2\Sigma_u^+$	0	$D_{\infty h}$ $^1\Sigma_g^+$		0.836(6)[d]		0.88(2)[d]
$AgCu_2^-$ $C_{\infty v}$ $^1\Sigma^+$	0	C_s $^2A'$	2.11	<2.32	2.37	2.39(5)
			1.78[b]			
			1.21/1.14[c]			
$AgCu_2^-$ $D_{\infty h}$ $^1\Sigma_g^+$	0.11		2.00		2.33	
	0.10[b]		1.68[b]			
			1.11/1.04[c]			
Ag_2Cu^- $D_{\infty h}$ $^1\Sigma_g^+$	0	C_{2v} $^2B_2$	2.18	<2.34	2.33	2.41(5)
			1.78[b]			
			1.80/1.86[c]			
Ag_2Cu^- $DC_{\infty v}$ $^1\Sigma^+$	0.09		2.09		2.37	
	<0.01[b]		1.77[b]			
			1.79/1.85[c]			
Ag_3^- $D_{\infty v}$ $^1\Sigma_g^+$	0	C_{2v} $^2B_2$		<2.37[d]		2.43(1)[d]
Cu_3^- $D_{\infty v}$ $^1\Sigma_g^+$	0	C_{2v} $^2B_2$		<2.27[d]		2.37(1)[d]

[a]Comparisons of calculated ADEs and VDEs with experimental measurements are shown. Numbers in parentheses are experimental uncertainties in the last digit. They are estimated by the products of kinetic energies of photoelectrons and the resolution of the apparatus in that range. [b]Reference 12. [c]Reference 15. [d]Reference 38.

Table 2. Comparing the Experimental Spectroscopic Constants of $AgCu^-$ and AgCu with the Results from Calculations[j]

system	r_e (Å) exptl	r_e (Å) calcd	ω_e (cm^{-1}) exptl	ω_e (cm^{-1}) calcd
$AgCu^-$ $^2\Sigma^+$	2.487(10)	2.485	191(15)	181
		2.622[a]		137[a]
Ag_2^- $^2\Sigma_u^+$	~2.611[b]		145(10)[b]	
Cu_2^- $^2\Sigma_u^+$	2.343(7)[b]		196(15)[b]	
AgCu $^1\Sigma^+$	2.373[c]	2.376	231.8[i]	225
		2.464[a]		229[d]
		2.378[d]		235[g]
		2.326[e]		193[a]
		2.338[f]		
		2.40[g]		
		2.40[h]		
Ag_2 $^1\Sigma_g^+$	2.480[b]		192.4[b]	
Cu_2 $^1\Sigma_g^+$	2.219[b]		266.4[b]	

[a]Reference 12. [b]Reference 38. [c]Reference 13. [d]Reference 39. [e]Reference 22. [f]Reference 15. [g]Reference 23. [h]Reference 24. [i]Reference 17. [j]Numbers in parentheses are experimental uncertainties in the last digit.

cm^{-1} (or 2.58 eV) higher than the ground state AgCu $^1\Sigma^+$. Taking the 0.93 eV energy difference between the ground state AgCu $^1\Sigma^+$ and $AgCu^-$ $^2\Sigma^+$ into account, the excited state AgCu $^1\Sigma^+$ is 3.51 eV higher than the ground state of $AgCu^-$. This energy value is higher than 355 nm photon (3.496 eV), so this state does not appear in the spectrum of Figure 1a. On the other hand, the first excited state AgCu $^3\Sigma^+$ corresponding to the A band in Figure 1a was not observed in previous experiments with use of absorption or emission spectroscopy, since the transitions between this state and the ground state AgCu $^1\Sigma^+$ are spin-forbidden.

The frequency and bond length of $AgCu^-$ are first determined by experiment. At the same time, the obtained frequency of AgCu is consistent with the value previously predicted by using emission or absorption spectroscopy.[13,17] As shown in Table 2, the calculated results of $AgCu^-$ and AgCu are in good agreement with the above experimental ones. The identification of 0←0 transition for the X band of $AgCu^-$ in Figure 1b leads to precise determination of its ADE or electron affinity (EA) of AgCu (0.93 eV). This allows us to predict the dissociation energy (D_0) of $AgCu^-$ using a thermodynamic cycle

$$D_0(AgCu^-) = D_0(AgCu) - EA(Ag) + EA(AgCu) \quad (1)$$

The reported D_0 (AgCu) and EA (Ag) are 1.76 eV[16] and 1.30 eV,[40] respectively. Therefore the dissociation energy from $AgCu^-$ to Ag^- and Cu is about 1.39 eV. The Ag−Cu bond in $AgCu^-$ is weaker than that in AgCu, which is due to the fact that the extra electron in $AgCu^-$ is on an antibonding orbital. From the data of $AgCu^-$ and the data of Ag_2^- and Cu_2^- from previous work[38] listed in Tables 1 and 2, we also find the following: the ADE or VDE of $AgCu^-$ is higher than that of Cu_2^- and lower than that of Ag_2^-, and the bond strength of $AgCu^-$ (or AgCu) is weaker than that of Cu_2^- (or Cu_2) and stronger than that of Ag_2^- (or Ag_2).

Comparing the calculated results with those from experiments, we find that many theoretical methods, including the strategy used in this research, the ab initio approach in ref 12, and the density functional theory methods in ref 15, more or less underestimated the ADE or VDE of $AgCu^-$. The calculated bond lengths here and those from a previous study with the CCSD (T) method[39] are within 0.005 Å range from the experimental values, whereas the values from other theoretical works[12,15,22−24] had large inaccuracies. As for the frequencies, the inaccuracies of our theoretical results and those from the CCSD (T) method[39] or the first-principles methods[23] are less

dx.doi.org/10.1021/jp307478x | J. Phys. Chem. A 2012, 116, 10365−10370

than 10 cm^{-1}. However, the values from ab initio approach in ref 12 seriously deviated from the experimental observation.

5.2. $AgCu_2^-$ and Ag_2Cu^-. The predicted lowest-lying structures for $AgCu_2^-$, Ag_2Cu^-, and their neutral counterparts in Figure 3 are consistent with those obtained in previous works using the ab initio method and DFT methods.[12,15] The energy separation between the lowest-lying structure and the closest-lying isomer is only 0.11 eV for $AgCu_2^-$ and 0.09 eV for Ag_2Cu^-. The theoretical VDEs for both two isomers of $AgCu_2^-$ or Ag_2Cu^- are close to the corresponding experimental values. The energy separations from the acute triangle and other isomers for neutral $AgCu_2$ or Ag_2Cu are slightly larger than those of the anions. The acute triangle is tentatively assigned to be the most stable neutral structure for both cases. For either of these dimers, photodetachment induces a major structural change from linear to triangle. This character is similar to what happens for Ag_3^- or Cu_3^-,[38] and is supported by the spectra in Figure 2 where there is a low-energy tail for each main peak.

Comparing experimental results of $AgCu_2^-$ or Ag_2Cu^- with those of Cu_3^- and Ag_3^- listed in Table 1, we find that the VDEs or the upper limit of ADEs increase with the content of Ag. The ADEs of Cu_3^- and Ag_3^- were estimated around 2.11 and 2.32 eV using their experimental VDEs and the energy differences between linear neutral structures and triangle ones from theoretical calculations.[38] Our calculated ADEs of $AgCu_2^-$ or Ag_2Cu^- are 2.11 and 2.18 eV, both of which are lower than that of Ag_3^- and equal to or higher than that of Cu_3^-. The theoretical values previously predicted by using the ab initio approach[12] and PBE and B3LYP[15] are obviously lower than the experimental observations. Considering the theoretical structures listed in Figure 3, we also find that the sequence of the bond lengths of Ag−Ag > Ag−Cu > Cu−Cu in dimers continues to apply on all isomers of Ag_2Cu^-, $AgCu_2^-$, and their neutral counterparts.

6. SUMMARY

Structures and electron properties of $AgCu^-$, $AgCu_2^-$, and Ag_2Cu^- are studied by using photoelectron imaging and theoretical calculations. Many important properties such as the adiabatic detachment energy of $AgCu^-$ (i.e., electron affinity of AgCu), the frequency and the bond length of $AgCu^-$, and the vertical detachment energies of all three anions are first obtained by experiments. The theoretical results predicted with use of PW91PW91 and CCSD (T) are close to these experimental ones. Analysis of the results indicates that the VDEs or ADEs of these clusters tend to increase with the content of silver and the bond lengths of Ag−Cu are shorter than those of Ag−Ag while longer than those of Cu−Cu. The characteristics revealed in these small clusters could also apply to large ones in this cluster family.

■ ASSOCIATED CONTENT

Supporting Information

Full ref 34. This material is available free of charge via the Internet at http://pubs.acs.org.

■ AUTHOR INFORMATION

Corresponding Author

*Tel.: +86-411-84379365. Fax: +86-411-84675584. E-mail: zctang@dicp.ac.cn (Z.T.) and xingxp@gucas.ac.cn (X.X.).

Notes

The authors declare no competing financial interest.

■ ACKNOWLEDGMENTS

This work was supported by the National Natural Science Foundation of China (Grant Nos. 21073186, 21103186, 21103226), the Ministry of Science and Technology of China, the Chinese Academy of Sciences, and the Present Fund of GUCAS (Grant No. Y05101GY00). The calculated results in this paper are obtained on the Deepcomp7000 of Supercomputing Center, Computer Network Information Center of Chinese Academy of Sciences.

■ REFERENCES

(1) Wang, L. M.; Pal, R.; Huang, W.; Zeng, X. C.; Wang, L. S. *J. Chem. Phys.* **2010**, *132*, 114306.
(2) Xing, X. P.; Tian, Z. X.; Liu, H. T.; Tang, Z. C. *Rapid Commun. Mass Spectrom.* **2003**, *17*, 1411−1415.
(3) Liu, X. J.; Li, B.; Han, K. L.; Sun, S. T.; Xing, X. P.; Tang, Z. C. *Phys. Chem. Chem. Phys.* **2009**, *11*, 1043−1049.
(4) Koszinowski, K.; Schroder, D.; Schwarz, H. *ChemPhysChem.* **2003**, *4*, 1233−1237.
(5) Joshi, A. M.; Tucker, M. H.; Delgass, W. N.; Thomson, K. T. *J. Chem. Phys.* **2006**, *125*, 194707.
(6) Harms, A. C.; Leuchtner, R. E.; Sigsworth, S. W.; Castleman, A. W. *J. Am. Chem. Soc.* **1990**, *112*, 5673−5674.
(7) Pal, R.; Cui, L. F.; Bulusu, S.; Zhai, H. J.; Wang, L. S.; Zeng, X. C. *J. Chem. Phys.* **2008**, *128*, 024305.
(8) Thomas, O. C.; Zheng, W. J.; Bowen, K. H. *J. Chem. Phys.* **2001**, *114*, 5514−5519.
(9) Ko, Y. J.; Shakya, A.; Wang, H. P.; Grubisic, A.; Zheng, W. J.; Götz, M.; Ganteför, G.; Bowen, K. H.; Jena, P.; Kiran, B. *J. Chem. Phys.* **2010**, *133*, 124308.
(10) Wang, L. M.; Bulusu, S.; Zhai, H. J.; Zeng, X. C.; Wang, L. S. *Angew. Chem., Int. Ed.* **2007**, *46*, 2915−2918.
(11) Negishi, Y.; Nakamura, Y.; Nakajima, A.; Kaya, K. *J. Chem. Phys.* **2001**, *115*, 3657−3663.
(12) Bauschlicher, C. W.; Langhoff, S. R.; Partridge, H. *J. Chem. Phys.* **1989**, *91*, 2412−2419.
(13) Bishea, G. A.; Marak, N.; Morse, M. D. *J. Chem. Phys.* **1991**, *95*, 5618−5629.
(14) Bishea, G. A.; Arrington, C. A.; Behm, J. M.; Morse, M. D. *J. Chem. Phys.* **1991**, *95*, 8765−8778.
(15) Kilimis, D. A.; Papageorgiou, D. G. *Eur. Phys. J. D* **2010**, *56*, 189−197.
(16) Ackerman, M.; Stafford, F. E.; Drowart, J. *J. Chem. Phys.* **1960**, *33*, 1784−1789.
(17) Joshi, K. C.; Majumdar, K. *Proc. Phys. Soc., London* **1961**, *78*, 197−200.
(18) James, A. M.; Lemire, G. W.; Langridgesmith, P. R. R. *Chem. Phys. Lett.* **1994**, *227*, 503−510.
(19) Cheeseman, M. A.; Eyler, J. R. *J. Phys. Chem.* **1992**, *96*, 1082−1087.
(20) Zhao, B.; Lu, H. Y.; Lombardi, J. R. *Chem. Phys. Lett.* **2003**, *375*, 425−428.
(21) Partridge, H.; Bauschlicher, C. W.; Langhoff, S. R. *Chem. Phys. Lett.* **1990**, *175*, 531−535.
(22) Jiang, Z. Y.; Lee, K. H.; Li, S. T.; Chu, S. Y. *Phys. Rev. B* **2006**, *73*, 235423.
(23) Li, S. F.; Shao, Z.; Han, S.; Xue, X.; Wang, F.; Sun, Q.; Jia, Y.; Guo, Z. X. *J. Chem. Phys.* **2009**, *131*, 184301.
(24) Lou, X.; Gao, H.; Wang, W.; Xu, C.; Zhang, H.; Zhang, Z. *J. Mol. Struct.: THEOCHEM* **2010**, *959*, 75−79.
(25) Wu, X.; Qin, Z. B.; Xie, H.; Cong, R.; Wu, X. H.; Tang, Z. C.; Fan, H. J. *J. Chem. Phys.* **2010**, *133*, 044303.
(26) Eppink, A.; Parker, D. H. *Rev. Sci. Instrum.* **1997**, *68*, 3477−3484.
(27) Dribinski, V.; Ossadtchi, A.; Mandelshtam, V. A.; Reisler, H. *Rev. Sci. Instrum.* **2002**, *73*, 2634−2642.

(28) Perdew, J. P.; Chevary, J. A.; Vosko, S. H.; Jackson, K. A.; Pederson, M. R.; Singh, D. J.; Fiolhais, C. *Phys. Rev. B* **1992**, *46*, 6671−6687.
(29) Peterson, K. A.; Puzzarini, C. *Theor. Chem. Acc.* **2005**, *114*, 283−296.
(30) Figgen, D.; Rauhut, G.; Dolg, M.; Stoll, H. *Chem. Phys.* **2005**, *311*, 227−244.
(31) Xie, H.; Xing, X. P.; Liu, Z. L.; Cong, R.; Qin, Z. B.; Wu, X.; Tang, Z. C.; Fan, H. J. *J. Chem. Phys.* **2012**, *136*, 184312.
(32) Xie, H.; Xing, X. P.; Liu, Z. L.; Cong, R.; Qin, Z. B.; Wu, X.; Tang, Z. C.; Fan, H. J. *Phys. Chem. Chem. Phys.* **2012**, *14*, 11666−11672.
(33) Bartlett, R. J.; Musial, M. *Rev. Mod. Phys.* **2007**, *79*, 291−352.
(34) Frisch, M. J.; Trucks, G. W.; Schlegel, H. B.; Scuseria, G. E.; Robb, M. A.; Cheeseman, J. R.; Scalmani, G.; Barone, V.; Mennucci, B.; Petersson, G. A. et al. *Gaussian 09*, Revision A02; Gaussian, Inc.: Wallingford, CT, 2009.
(35) Ervin, K. M. PESCAL, FORTRAN program, 2010; Ervin, K. M.; Ramond, T. M.; Davico, G. E.; Schwartz, R. L.; Casey S. M.; Lineberger, W. C. *J. Phys. Chem. A* **2001**, *105*, 10822−10831.
(36) Surber, E.; Mabbs, R.; Sanov, A. *J. Phys. Chem. A* **2003**, *107*, 8215−8224.
(37) Grumbling, E. R.; Sanov, A. *J. Chem. Phys.* **2011**, *135*, 164302.
(38) Ho, J.; Ervin, K. M.; Lineberger, W. C. *J. Chem. Phys.* **1990**, *93*, 6987−7002.
(39) Kello, V.; Sadlej, A. J. *J. Chem. Phys.* **1995**, *103*, 2991−2999.
(40) Bilodeau, R. C.; Scheer, M.; Haugen, H. K. *J. Phys. B: At., Mol. Opt. Phys.* **1998**, *31*, 3885−3891.